



Electron impact partial ionization cross section and thermal rate coefficients of gaseous refrigerants

Suriyaprasanth S  and Dhanoj Gupta ‡ 

Department of Physics, School of Advanced Sciences, Vellore Institute of Technology, Katpadi, Vellore - 632014, Tamil Nadu, India

E-mail: suriyaprasanth.s@vit.ac.in, dhanoj.gupta@vit.ac.in

Abstract. We have calculated the electron impact partial and total ionization cross sections of important gaseous targets, such as Trifluoromethane (CHF_3), 1,1,1,2-Tetrafluoroethane ($\text{C}_2\text{H}_2\text{F}_4$) or R134a, 1,1,1-Trifluoroethane ($\text{C}_2\text{H}_3\text{F}_3$) or R143a, 1,1,1-Trifluoropropane ($\text{C}_3\text{H}_5\text{F}_3$) or R263fb, and 3,3,3-Trifluoropropene ($\text{C}_3\text{H}_3\text{F}_3$) or R1243zf using the binary encounter Bethe model and its variants. The corresponding rate coefficients are calculated for total and partial ionization cross sections using the Maxwell's velocity distribution function. Our data for partial and total ionization along with the rate coefficient showed good agreement with the existing data in the literature. The targets studied are important for plasma applications and are used in gas-based detectors at high-energy physics experiments.

Keywords: electron impact ionization cross section, BEB model, partial electron impact ionization cross section, ionization rate coefficients, thermal rates, gaseous refrigerants, R134a, R143a. Submitted to: arXiv

1. Introduction

The study of electron and positron scattering is of fundamental importance in many areas of physics and engineering such as plasma modelling, aeronomy, studying radiation damage in living cells, modelling electron transport in the matter, and many others [1, 2, 3, 4]. In the present work, we mainly focus on exploring the electron inelastic scattering on neutral molecules used as refrigerants in household appliances and as gaseous detectors in high-energy physics experiments. These refrigerants used in gas-based detectors are inevitable as the gases containing fluorine atoms provide optimal performance while detecting elementary particles [5]. However, researchers are now striving to eliminate the use of these gases due to their severe environmental impact. For example, experiments like the mini-iron calorimeter (mini-ICAL), which uses resistive plate chambers (RPC), rely on a quenching medium mixture of R134a, isobutane, and SF₆ to achieve precise time resolution and efficient avalanche operation [6]. Similarly, the Compact Muon Solenoid (CMS) experiment at the CERN also uses an RPC for the detection of charged particles which also uses the same R143a mixture in their RPCs. Although R143a gas is suitable for detectors, its global warming potential (GWP) is quite high, raising concern for its usage [5]. To certify a gas as a viable alternative, we must examine its electron swarm parameters, effective ionization coefficients, transport properties such as drift velocity, Townsend coefficients, attachment coefficients and both longitudinal and transverse diffusion coefficients that can be studied by numerically solving the Boltzmann's equation or using the Monte-Carlo simulation. Popular and well-tested suites used to perform such studies are the `PyBoltz` code

[7], its predecessor `MagBoltz` code [8] and the recent `ThunderBoltz` which is a 0D Direct Simulation Monte-Carlo (DSMC) code [9] also requires cross section set to perform plasma transport studies. Before delving into these studies, it is crucial to understand how the gas behaves when exposed to charged particles such as electrons and positrons. Our aim is to provide the fundamental electron scattering cross sections for some of the important gases used in high-energy physics experiments such as the electron impact total ionization cross sections (TICS) and partial ionization cross sections (PICS). In the absence of the PICS data, only the TICS is being used to perform the studies on calculating swarm parameters [10]. Hence, including the dissociative ionization channels will certainly improve the accuracy of the calculations of swarm parameters. Moreover, the data obtained from these collision processes are used to calculate the electron transport parameters using the `bolsig+` [11], in a weakly ionized gas medium. The molecules that are investigated in this article are the Trifluoromethane (CHF₃) also commonly known as Fluoroform is found to have zero GWP and zero ozone depletion potential (ODP), Whereas the 1,1,1,2-Tetrafluoroethane (CH₂FCF₃) commonly known as the R134a has a GWP of 1430 and zero ODP. 1,1,1-Trifluoroethane (C₂H₃F₃) also identified as R143a has a GWP of 4300, however, it has zero ODP. The GWP and ODP of 1,1,1-Trifluoropropane (C₃H₅F₃) and 3,3,3-Trifluoropropene (C₂H₃CF₃) are unavailable in the literature. In the present article, we have calculated the TICS of the neutral molecule and PICS of the prominent cationic fragments whose appearance energies and relative abundance are available in the literature. The cross section obtained is used to calculate the corresponding rate coefficients for TICS and

PICS using the Maxwell-Boltzmann distribution. The article’s structure is as follows: section 2 describes the models applied to calculate the PICS; section 3 discusses the calculation of rate coefficients for ionization processes and in section 4 we have discussed the results and findings of the present study.

2. BEB Model for electron

The binary encounter Bethe (BEB) model is a widely used formalism to calculate the electron and positron impact ionization cross sections of atoms, molecules, and ions. Many works [12, 13] have employed the BEB model to predict the TICS and PICS by electron impact of the molecular targets. The model generally works by calculating the ionization cross sections of each occupied orbital present in the molecule and then summing it up to provide the TICS for electron impact as given in Equation (1).

$$\sigma_{TICS}(E) = \sum_i^N \sigma_i(E) \quad (1)$$

The simplified BEB model introduced by Kim and Rudd [14] is defined as,

$$\sigma_i^{BEB}(E) = \frac{S_i}{(t_i + u_i + 1)/n} \left[\frac{Q_i \ln t_i}{2} \left(1 - \frac{1}{t_i^2} \right) + (2 - Q_i) \left\{ \left(1 - \frac{1}{t_i} \right) - \frac{\ln t_i}{t_i + 1} \right\} \right] \quad (2)$$

Here, t_i, u_i and S are the reduced variables which are defined as,

$$S_i = 4\pi a_0^2 N \left(\frac{R}{B} \right)^2, \quad u_i = \frac{U}{B}, \quad t_i = \frac{E}{B} \quad (3)$$

In the present calculation, a_0 and R represent the Bohr radius (0.52918 Å), and the Rydberg constant (13.6057 eV). The differential oscillator strength, Q_i is set to unity according to the simplified BEB model. The U and B

are the orbital kinetic and binding energy of the molecule which is obtained by performing quantum chemistry calculations. The scaling factor (n) is fixed to unity for all the molecular orbitals due to the presence of lighter atoms ($Z < 10$) in the molecular targets. If there exists an atom with ($Z > 10$), (n) is set as the principal quantum number of the dominant atom, which is determined by performing Mulliken population analysis ([13] and references within). N is the occupation number of the orbital, and the incident electron kinetic energy is represented by E . The orbital parameters for a molecule were calculated using a similar method applied in our previous work [13], where we have optimized the geometries of the molecule by applying the density functional theory (DFT) with the functional (ω B97XD) and with the aug-cc-PVTZ (aVTZ) basis set. Once the stable geometry is obtained then the energies are calculated using the Hartree-Fock (\mathcal{HF}) approximation using the same basis set (aVTZ). In Figure 1, the structure of the molecular targets sketched from the SMILES code from the Protein Data Bank’s online chem sketch tool [15] is presented. The \mathcal{HF} method generally overestimates the binding energies a little which leads to the underestimation of the theoretical TICS when compared with the experimental cross sections. However, the calculated TICS is found to lie between 10 % and 15 % uncertainty when compared with the experiment [12].

2.1. mBEB model

To calculate the PICS we need information such as the fragmentation pathway, dissociation energy/appearance energy (φ), and the electron impact mass spectrum (EIMS). We will be discussing two methods to cal-

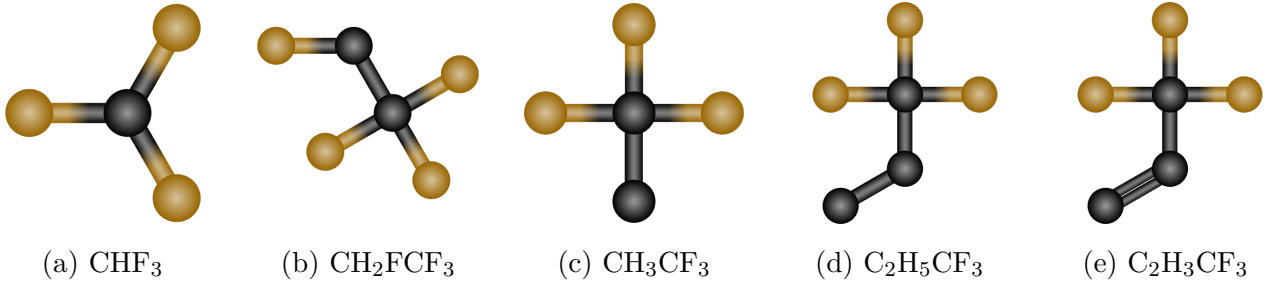


Figure 1: The structures of the molecular targets: a) Trifluoromethane b) 1,1,1,2-Tetrafluoroethane (R134a) c) 1,1,1-Trifluoroethane (R143a), d) 1,1,1-Trifluoropropane, e) 3,3,3-Trifluoropropene

calculate the PICS, the mass spectrum dependence (MSD) method and the modified BEB (mBEB) method. In the mBEB model, the cations formed due to dissociative ionization by electron or positron impact can be distinguished through φ . The ionization energy of the molecule is obtained from the highest occupied molecular orbital (HOMO) of the neutral parent molecule ($IP_{koopman's} = -\text{HOMO}$). To enable the mBEB model to calculate the PICS for all cations using AE and experimental BR, a minor adjustment to the binding energies of the occupied orbitals of the neutral parent molecule is required. This is facilitated via summing the difference (Δ) between the neutral parent molecule's IE and the (φ) of the fragment, ($\Delta = IE - \varphi$) to all the values of the orbital binding energies of the parent molecule ($B' = B + \Delta$). This correction replaces the HOMO of the cation by its φ . The mBEB method is defined as,

$$\sigma_i^{mBEB}(E) = \frac{S'_i}{(t'_i + u'_i + 1)/n} \left[\frac{Q_i \ln t'_i}{2} \left(1 - \frac{1}{t'^2_i} \right) + (2 - Q_i) \left\{ \left(1 - \frac{1}{t'_i} \right) - \frac{\ln t'_i}{t'_i + 1} \right\} \right] \quad (4)$$

The modified reduced variables are as follows,

$$S'_i = 4\pi a_0^2 N \left(\frac{R}{B'} \right)^2, \quad t'_i = \left(\frac{E}{B'} \right), \quad u'_i = \frac{U}{B'} \quad (5)$$

Then the PICS is calculated as shown in

Equation (6),

$$\sigma^{PICS}(E) = \Upsilon_i(E_r) \times \sigma_i^{mBEB}(E) \quad (6)$$

Υ_i is the scaling factor which is determined from the ratio of the experimental BR vs the theoretical BR [see Equation (9)]. The BR obtained via the experimental EIMS data is the experimental BR (Γ_i^{Exp}) which is estimated as seen in Equation (7). In experiments, the EIMS data is measured at one incident energy or reference energy (E_r) which can either be at 70 eV, 100 eV or 125 eV according to the user's choice of the experimental parameter,

$$\Gamma_i^{Exp}(E_r) = \frac{R(E_r)}{T(E_r)} \quad (7)$$

Here the $R(E_r)$ is the relative abundance of the cation and the $T(E_r)$ is the total abundance, the sum of all $R(E_r)$ of cations. This electron impact mass spectrum can also be generated theoretically using quantum chemical mass spectrometry (QCxMS)[16], when the experimental EIMS data are scarce. The theoretical BR (Γ_i^{Theo}) is the ratio of the PICS calculated with the mBEB model before introducing the scaling factor,

$$\Gamma_i^{Theo}(E_r) = \frac{\sigma_i^{mBEB}(E_r)}{\sigma_i^{BEB}(E_r)} \quad (8)$$

Then the scaling factor $\Upsilon_i(E_r)$ is obtained by

$$\Upsilon_i(E_r) = \frac{\Gamma_i^{Exp}(E_r)}{\Gamma_i^{Theo}(E_r)} \quad (9)$$

There is also another method that was implemented by Huber et al. [17] which can be used to calculate the BR using the appearance energy or the dissociation energy which we have explained in our recent work [13]. The MSD method to compute PICS is discussed in the next section.

2.2. MSD method

Usually, the branching ratio is a single-valued quantity in the above mBEB method. But, here we make it incident energy-dependent and thus continuous throughout the range of the incident kinetic energy (E). Here we also need the information on the experimental BR.

$$\Gamma_i^{MSD}(E) = \begin{cases} 0 & \text{if } E < \varphi \\ \Gamma_i(E_r) \left[1 - \left(\frac{\varphi}{E} \right)^\nu \right] & \text{if } E \geq \varphi \end{cases} \quad (10)$$

The value ν is set to be 1.5, which is the control parameter suggested by Janev et al. [18] More details about this method can be obtained from the works of Graves [19], Huber[17], and in our recent work[13]. Another important component of the BR is that its sum always yields unity, irrespective of the method used. In a few cases where we might not know all the fragmentation pathways of a molecule, the sum can be less than unity. Once we perform this BR check, we can calculate the PICS using the MSD method.

$$\sigma^{PICS}(E) = \Gamma_i^{MSD}(E) \times \sigma_i^{BEB}(E) \quad (11)$$

3. Ionization Rate coefficients

In thermal plasmas, the electron's velocity distribution function is considered as the Maxwellian electron distribution function for isotropic velocities for temperature.

$$f(v, T_e) = 4\pi v^2 \left(\frac{m_e}{2\pi k_B T_e} \right)^{3/2} \exp \left(-\frac{m_e v^2}{2k_B T_e} \right) \quad (12)$$

Where, v is the electron velocity, m_e is the mass of the electron and k_B is the Boltzmann constant. The rate coefficient is derived by averaging the cross sections over the Maxwellian electron velocity distribution (MVD) as follows.

$$k(T_e) = \int_0^\infty \sigma(v) f(v, T_e) v dv \quad (13)$$

$\sigma(v)$ is the ionization cross sections. The calculated ionization rate coefficients are in the temperature range of 1 eV and 10 eV which is then fitted using the Arrhenius equation till 100 eV temperature,

$$k = AT_e^n \exp \left(\frac{-E_{act}}{T_e} \right) \quad (14)$$

AT_e^n is the temperature dependent pre-factor in cm^3s^{-1} , E_{act} is the activation energy in eV and T_e is the electron temperature in eV. E_{act} , A , n are the fitting parameters. The best-fit parameters are given in the tables 2 to 7.

4. Results and Discussion

In this part, we show the PICS and TICS calculated for all the molecular targets along with their corresponding rate coefficients. Since the BEB cross section is sensitive to the values of the valence shell orbitals, the HOMO energies obtained in our calculations using the \mathcal{HF} and DFT approach are presented along with the literature values in table 1. Each subsection discussed below contains the branching ratio, PICS, TICS, and the corresponding rate coefficient for PICS and TICS for each of the targets studied.

4.1. Trifluoromethane

CHF_3 molecule has been very well studied over several years for ionization experimentally. Here we would like to revisit them and also theoretically calculate the PICS as they

Table 1: Vertical, Adiabatic, HOMO, Ionization energies of molecules

Molecular formula	Name	HOMO (eV)		Ionization potential (eV)
		DFT	\mathcal{HF}	Literature
CHF ₃	Trifluoromethane	13.40	16.31	13.86[20], 14.8[21], 15.5 ^b [22]
CH ₃ CF ₃	1,1,1 Trifluoroethane	12.58	15.39	13.3 ± 0.1 [23], 13.8 ^b [22]
C ₂ H ₅ CF ₃	1,1,1 Trifluoropropane	10.69	11.42	–
C ₂ H ₃ CF ₃	3,3,3 Trifluoropropane	12.16	14.22	11.24[24]
CH ₂ FCF ₃	1,1,1,2 Tetrafluoroethane	12.48	15.16	13.10 ± 0.17[25], 13.19[25], 12.25 ^a [26]13.96 ^b [26]

^aAdiabatic IE, ^bVertical IE

are not available in the literature and the corresponding rate coefficients for ionization and dissociative ionization are also computed. Goto and co-workers [27] had experimentally measured the TICS and PICS of CHF₃ using the dual electron beam apparatus coupled with a quadrupole mass spectrometer (QMS). They provided the reaction channels for neutral dissociation and also measured the threshold energy. It was the first time where the cross sections were reported for individual cations along with their AEs, until then only the dominant cations CF_{*x*}⁺ : *x* = 1, 2, 3 and combined cross sections of two or more cations were reported [28, 29]. Later, Jiao et al [30] also provided the experimental PICS and TICS for the CF_{*x*}⁺ : *x* = 1, 2, 3 along with CHF₂⁺ using the Fourier transform mass spectrometry (FTMS) with a cubic ion cyclotron resonance (ICR) trap cell. Iga and colleagues [31] also provided the PICS, TICS, and the mass spectrum for the same. The measurements were performed using the time-of-flight mass spectrometer (TOFMS) along with the QMS for identification of *m/z* values of ions, the mass spectrum was recorded at 200 eV incident energy. Their mass spectrum shows that the

base peak was from CHF₂⁺ ion and the other peaks are due to ions of CF_{*x*}⁺ (*x* = 1, 2, 3), C⁺ and F⁺. The PICS of these cations detected in the mass spectrums were measured from the ionization threshold till 1 keV, and cross sections of CF₃⁺ and F⁺ ions were measured individually. The other contributions of PICS are bundled cross sections of the ions (CHF₂⁺ + CF₂⁺), (CHF⁺ + CF⁺) and the (C⁺ + CH⁺), their findings agree very well with Goto et al [27]. Torres et al [32] experimentally measured the PICS using the linear double-focusing time-of-flight apparatus where the electron kinetic energies were varied from 0 eV to 100 eV, along with their AEs.

On the theoretical front, Onthong[33] working with Deutsch and Märk used the Deutsch–Märk (DM) model to calculate the TICS, their data had a very good comparison with the Iga et al [31]. Torres et al [34] has extensively performed TICS calculations using parameters from various levels of theory such as the Møller-Plesset second-order perturbation (MP2), Møller-Plesset fourth-order perturbation (MP4), Configuration interaction singles and doubles (CISD), Coupled cluster (CC) and \mathcal{HF} for several fluoromethanes in-

cluding CHF_3 . They replaced the HOMO energy with an experimental ionization threshold value for better results from the BEB method. In their work, they also compared the cross-sections calculated using the modified additivity rule (MAR), DM formalism, and the BEB method. It is well known that the MAR would overestimate the TICS and the DM method also falls short in low energy regions. The calculation using the BEB model included the optical oscillator strengths (OOS) of the ground state of the Hydrogen atom as an approximation rather than using the OOS of target molecules. The OOS are quite cumbersome to calculate. In our case, we have used the simplified BEB model which does not require the OOS.

In our present work, we have considered the AEs from the work of Torres et al [32] for each cation which can be seen in Table 3. We would also require the mass spectrum for calculating the BR. The electron impact mass spectrum data is provided by Peko et al [35] measured at the incident energy 70 eV, where they have detected most of the fragments but have missed detecting the HF^+ fragment. In our calculations, we have chosen the EIMS data from the NIST Webbook [22], for calculating the BRs and shown in Table 3. We have presented the BR calculated using the MSD method and the BR calculated from the experimental branching ratios in Figure 4a. Later Christophorou and Olthoff [36] provided the recommended TICS and PICS by compiling the PICS of Jiao et al [30], Iga et al [31] and Torres et al [32] altogether by fitting, summing and normalizing the cross sections for each energy. It can be seen in Figure 2, that the recommended cross sections and our calculations match very well for most stable ions. It was also mentioned by Torres et al that the uncertainties for the

lighter ions ($m/z < 20$ amu) are higher (15% to 20%) whereas the heavier ions tend to have an uncertainty of less than 10%. The recommended data by Christophorou et al [36] does not have any uncertainties. Recently, Kawaguchi et al. [37] used the inverse swarm method to calculate the PICS from 85 eV to 1 keV using the TICS presented by Kim et al.

From Figure 2, it can be seen that for lighter fragments such as the CH^+ and F^+ , there is quite a lot of disagreement of our cross sections when compared with the literature data. For all the other fragments our theoretical cross sections are similar to the literature values. We have calculated the ionization and dissociation rates in Figure 3, where we have used the cross sections calculated with the MSD method as an input since it had a better agreement of cross sections with the literature data as shown in our previous work [13] as well as in the current work. Morgan-Winstead-McKoy[38] calculated the dissociation rates for the fragments CF_x^+ : $x = 1, 2, 3$ and CHF_y^+ : $y = 2, 3$ in the range of 0 eV and 15 eV. Later Bose and co-workers calculated the rate coefficients and fitted them with the Arrhenius equation, provided with the necessary parameters. In Table 2, we have compared the fitting parameters calculated using Scipy's curve fit function [39] with the literature values.

4.2. 1,1,1,2-Tetrafluoroethane

Here we discuss about the molecule 1,1,1,2-Tetrafluoroethane which is a quite well-studied target with the common name R134a. A plethora of data is found in the literature. The recent one is by Marnik Metting van Rijn et al has revisited the electron scattering cross section of R134a and performed swarm stud-

Table 2: The calculated fitting parameters of the Arrhenius equation to calculate rate constants for CHF₃ molecule compared with the data shown by Bose et al [40]

Cation	A (10 ⁻¹⁰ cm ³ s ⁻¹ eV ⁻ⁿ)		n		E _{act} (eV)	
	Present	Literature	Present	Literature	Present	Literature
CF ₃	22.8	313.8[40]	1.288	-0.2366[40]	14.5532	—
CHF ₂	17.4	184.5[38], 48.59[40]	1.2142	0.4022[38], -0.1043[40]	15.7526	17.08[38], 19.576[40]
CF ₂	6.37	242.9[38], 33.29[40]	0.9797	0.2566[38], -0.0048[40]	19.3258	22.33[38] 19.542[40]
CHF	1.56	20.79[40]	0.9327	0.4581[40]	20.4678	—
CF	1.49	119.0[38], 64.37[40]	0.9224	0.1276[38], 0.2857[40]	20.6763	23.16[38], 19.474 [40]
HF	5.2	—	0.7968	—	28.55	—
F	2.04	—	0.6069	—	36.9257	—
CH	0.208	—	0.6955	—	29.7174	—
C	0.723	—	0.6484	—	33.6389	—
CHF ₃	21.1	103.3[38]	1.5084	0.3601[38]	13.2155	15.00[38]

Table 3: The Appearance Energy (AE), Branching ratios (BR), cross section's maximum value (σ), the values of pre-exponent (A), scaling term (n) and the activation energy (E_{act}) of Trifluoromethane (CHF₃)

m/z	Cation	AE (eV)	BR	σ (10 ⁻¹⁶ cm ²)	A(10 ⁻¹⁰ cm ³ s ⁻¹ eV ⁻ⁿ)	n	E _{act} (eV)
69	CF ₃	13.9 ± 0.6	0.49 263	2.2397	5.693	1.7021	14.3532
51	CHF ₂	15.7 ± 0.5	0.34 464	1.5561	6.183	1.5269	15.8342
50	CF ₂	19.5 ± 0.5	0.05 449	0.2423	2.317	1.5269	19.3377
32	CHF	20.7 ± 0.5	0.00 838	0.0371	4.368	1.1217	20.4676
31	CF	20.9 ± 0.5	0.18 548	0.8198	10.063	1.1072	20.6735
20	HF	28.8 ± 0.5	0.06 644	0.1605	5.196	0.7968	28.55
19	F	37.0 ± 0.5	0.01 286	0.0528	2.917	0.6547	36.8771
13	CH	29.9 ± 0.5	0.01 181	0.0502	1.786	0.7693	29.6736
12	C	33.8 ± 0.5	0.01 555	0.0649	2.968	0.7035	33.5933
70	CHF₃	13.860	—	4.7150	21.108	1.5084	13.2155

ies on the Pulsed Townsend apparatus experimentally and also used MAGBOLTZ to calculate parameters such as drift velocity and effective ionization co-efficient [10], a compre-

hensive set of cross sections of other molecular processes such as the elastic + rotational + momentum transfer, total elastic, vibrational and the ionization has been presented. Víctor

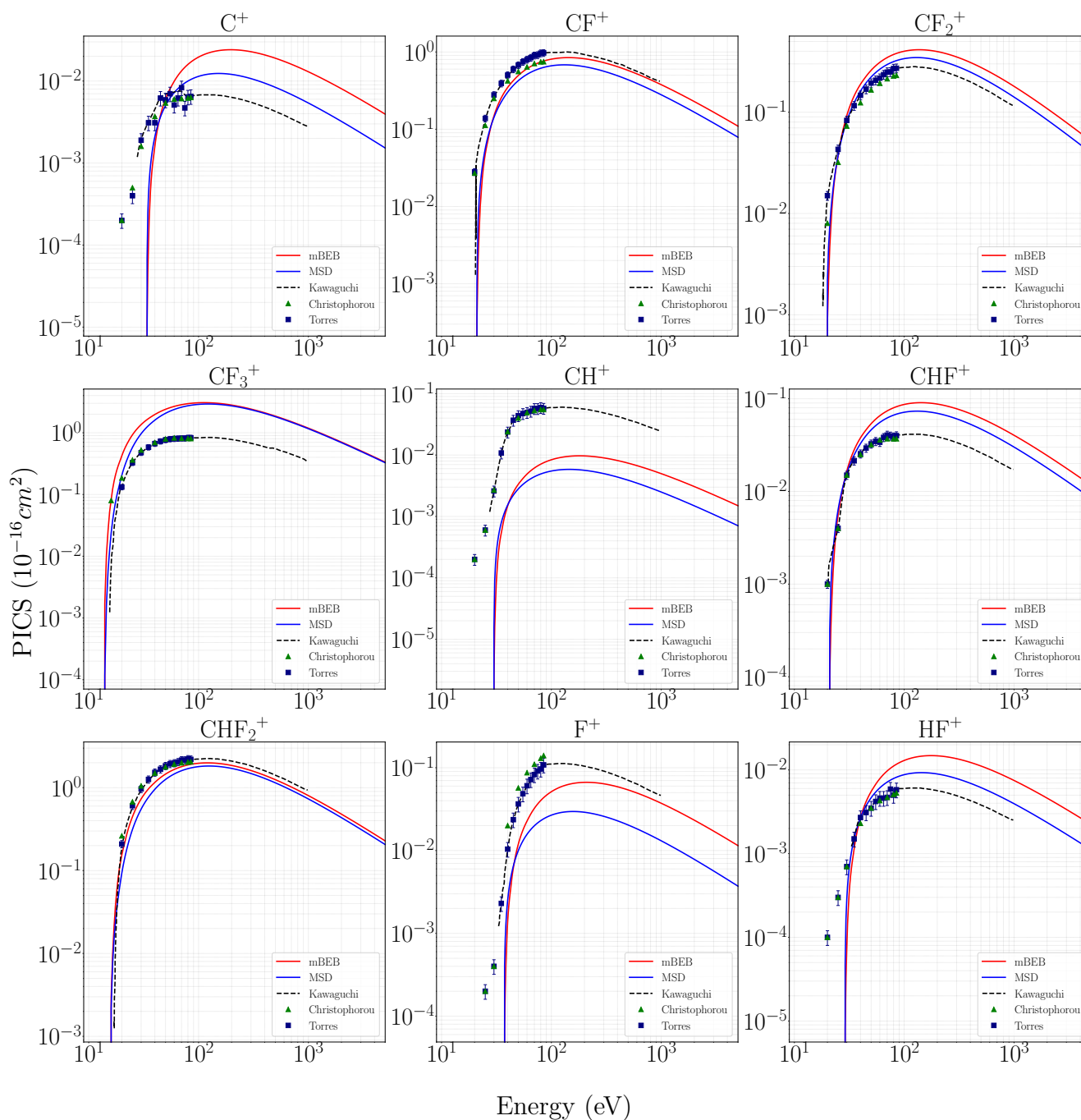


Figure 2: PICS of Trifluoromethane: cations detected in the EIMS, the blue solid line represents the calculated cross sections using the mBEB model, and the solid red line represents the calculated cross sections using the MSD method. the dotted lines represent the PICS presented by Kawaguchi et al [37], the green upright triangles represent the recommended cross sections by Christophorou et al [36] and the blue squares are the PICS by Torres et al [32].

S. A. Bonfim et al investigated the photodissociation and the several pathways in the pro-

duction of CHF_2^+ fragment (references within [41]), which had an RI of 4% in the study of

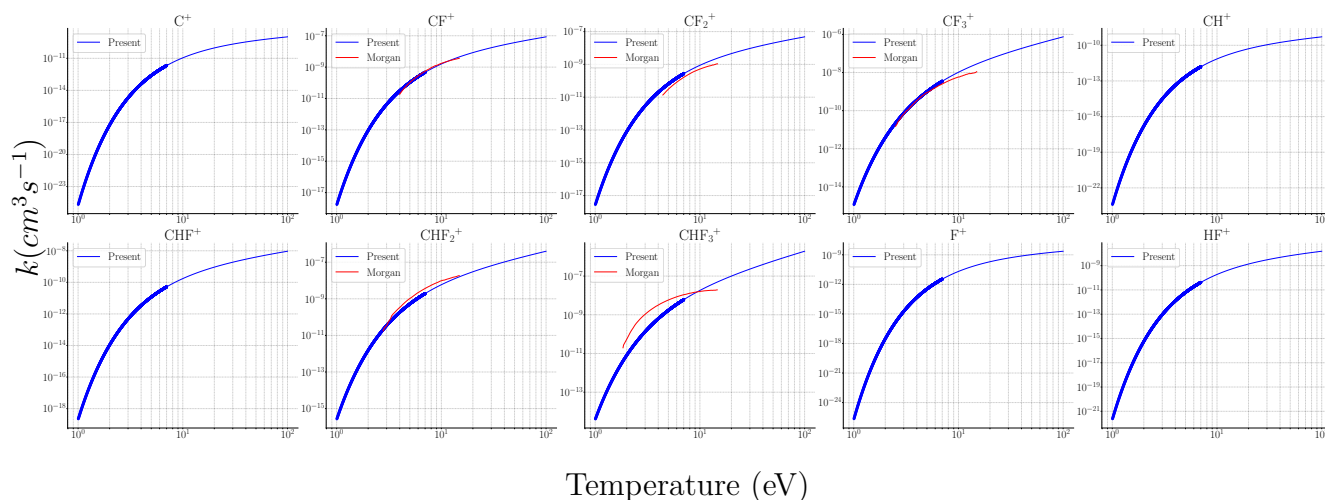


Figure 3: Ionization rates of Trifluoromethane: the blue solid lines represent the ionization rates, whereas the red solid lines represent the rates calculated presented by Morgan et al [38] in the range of 1 eV till 15 eV.

Pereira-da Silva [25] which used a Trochoidal electron monochromator (TEMs) coupled with an Orthogonal Reflectron Time-of-Flight Mass Spectrometer (OReToFMS) to determine the positive and negative ion formations. They also provided the mass spectrum and AEs for a few fragments which can be seen in Table 4. As usual, the most abundant fragment is CF_3^+ having AE as 13.39 eV. Several works [25, 42] have cited the vertical IE as 13.2 eV which was attributed to the NIST web book [22]. The vertical IE and the adiabatic IE were reported by Zhou et al [26] as 12.25 eV and 13.96 eV. Here we have calculated the PICS based on the mass spectrum and AEs presented by Pereira-da Silva [25] which is shown in Figure 5. The Figure 6a, shows the branching ratios, the solid lines represent the continuous BRs and the upright triangles represent the experimental BR. The fragments CHCF_2^+ (63) and CHF_2^+ (51) have the same RI which is the reason for the overlapping of the continuous BR in the high energy region. In Table 4, we have shown the BRs, cross sections, and the fitting parameters

for the rate coefficients. The rate constants for the TICS and PICS have been presented in Figure 6c. The TICS has been calculated using the parameters obtained from the \mathcal{HF} and DFT parameters. The HOMO values have been replaced with the literature values and the TICS profiles using various methods along with the literature data is shown in Figure 6b.

4.3. 1,1,1-Trifluoroethane

In the case of 1,1,1-Trifluoroethane, the mass spectrum and appearance energies were obtained from the work of Steele and Stone [24]. The AEs were measured using the modified Consolidated Electroynamics Corporation (CEC) 21-103 C mass spectrometer. Later Simme and Tschuikow-Roux [23] also measured the mass spectrum using the Varian Atlas CH-5 spectrometer and the appearance potential (AP) of the 1,1,1 Trifluoroethane molecule was calculated from the semilog plots of the iron current vs the electron voltage. This work has revisited the experiment and has measured the mass spectrum of three more

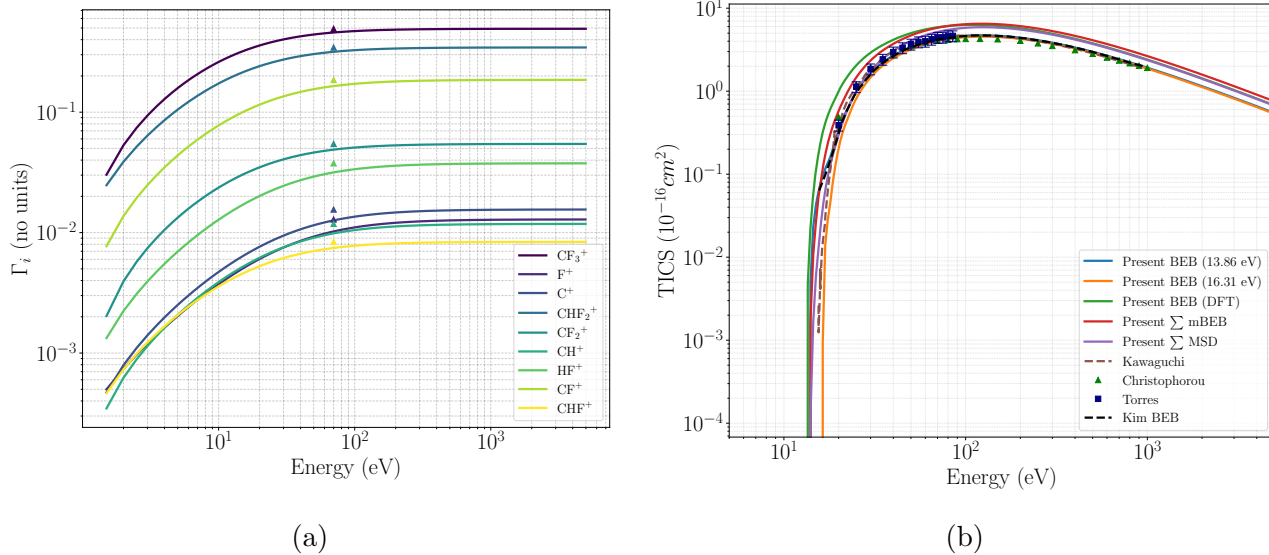


Figure 4: a) Branching ratios for the fragments of Trifluoromethane: The solid lines represent the branching ratios calculated for the MSD method, whereas the solid triangles denote the branching ratios calculated from the EIMS. b) Trifluoromethane TICS calculated using different methods, the solid blue line represents our calculated BEB TICS where the experimental first ionization energy was used, and the solid orange line shows the present BEB TICS calculated using HOMO energy obtained by HF approximation. The solid green line represents the TICS calculated from orbital parameters obtained using DFT. The red solid line shows the TICS which was the sum of all the PICS calculated from the mBEB model. The solid purple line shows the TICS which was the sum of all the PICS calculated from the MSD model. The dashed brown line represents the TICS from the work of Kawaguchi et al [37]. The solid upright triangles represent the recommended TICS from Christophorou et al [36]. The dashed black line represents the TICS calculated using the BEB method by Kim et al [34].

Table 4: The Appearance Energy (AE), Branching ratios (BR), cross section's maximum value (σ), the values of pre-exponent (A), scaling term (n) and the activation energy (E_{act}) of 1,1,1,2 Tetrafluoroethane (CF_3CH_2F)

m/z	Cation	AE (eV)[25]	BR	σ ($10^{-16}cm^2$)	$A(10^{-10}cm^3s^{-1} eV^{-n})$	n	E_{act} (eV)
101	CF_3CHF	14.56 ± 0.17	0.01 796	0.1217	0.4174	1.6013	15.013
83	CF_3CH_2	15.51 ± 0.11	0.10 778	0.7227	3.120	1.513	15.7732
69	CF_3	13.39 ± 0.10	0.59 880	4.0765	11.51	1.6793	14.2757
63	$CHCF_2$	16.99 ± 0.25	0.02 395	0.1607	1.005	1.3664	17.0944
51	CHF_2	14.03 ± 0.64	0.02 395	0.1626	0.5018	1.6434	14.6414
33	CH_2F	13.36 ± 0.17	0.15 568	1.0600	2.984	1.6802	14.262
102	CF_3CH_2F	13.10 ± 0.17	–	7.0535	34.29	1.4986	13.3273

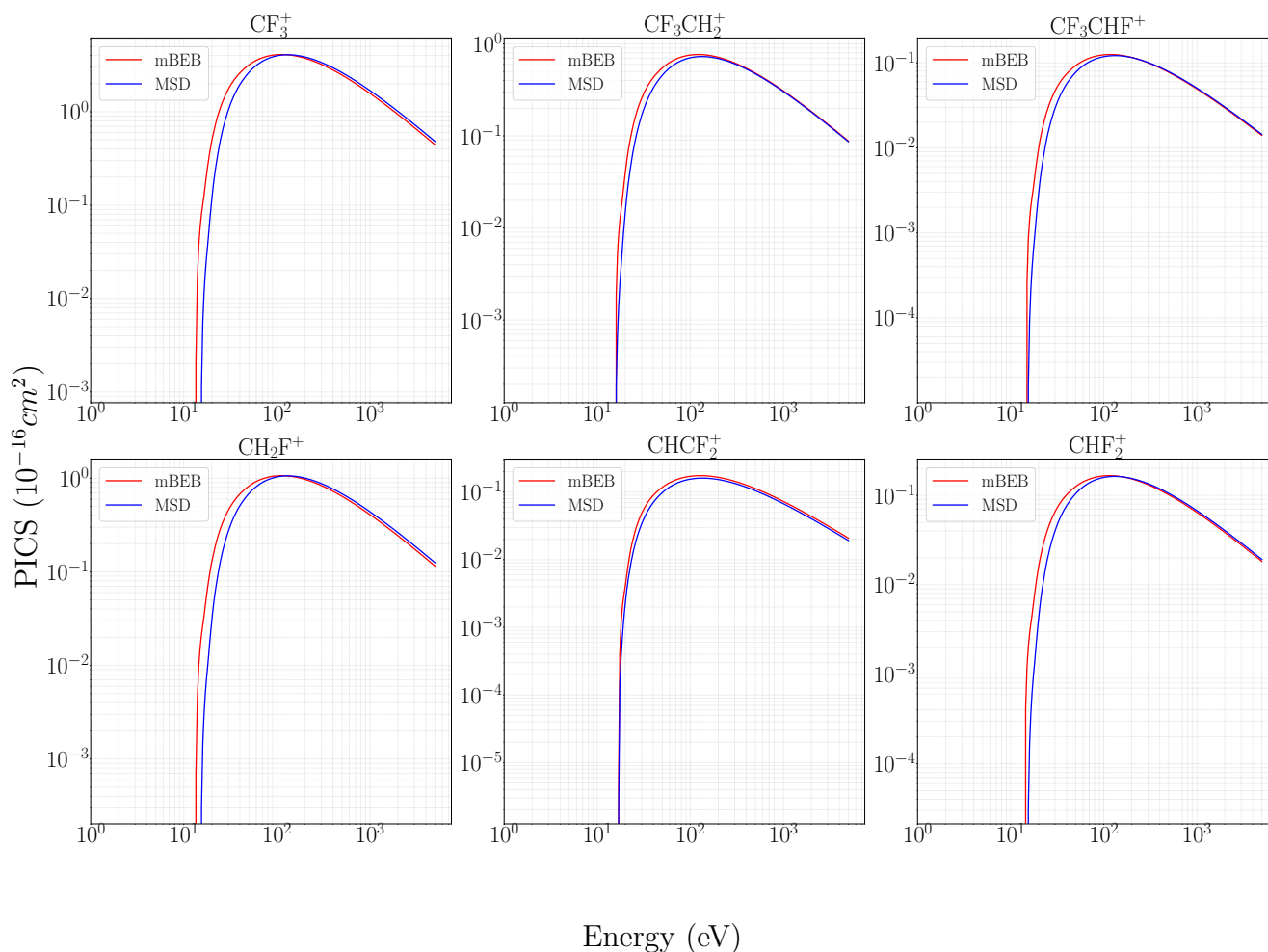


Figure 5: PICS of 1,1,1,2-Tetrafluoroethane: cations detected in the EIMS, the blue solid line represents the calculated cross sections using the mBEB model, and the solid red line represents the calculated cross sections using the MSD method

important cations that Steele and Stone did not detect; this includes fragments such as m/z : Cation – 84: CH_3CF_3 , 63: CHCF_2 , 51: CHF_2 and 31: CF . On the contrary, all these cations have relative abundances (RI) $< 5\%$. A cation of m/z of 14: CH_2 went undetected in their measurement. This cation was then detected by Steele and Stone which had RI of $< 5\%$. The shortcomings in the study of Simme and Tschuikow-Roux is that the APs were not measured for all the cations. Hence we have used the data provided by Steele and Stone [24] for RI and AEs of the cations. In

Table 5, we have shown the calculated BRs along with the PICS and the fitting parameters of the rate constants. In Figure 7, we have presented the PICS for the seven cationic fragments detected by Steele and Stone [24]. As the AEs were not provided for CH_3CF_3^+ , CHCF_2^+ , CHF_2^+ , and CF^+ , we could not calculate the PICS for these fragments that may be of interest as they induce further ion-ion, ion-atom, and ion-molecule processes in dense environments. We would also prescribe revisiting the study with the current instrumentation as they are quite sensitive and precise and

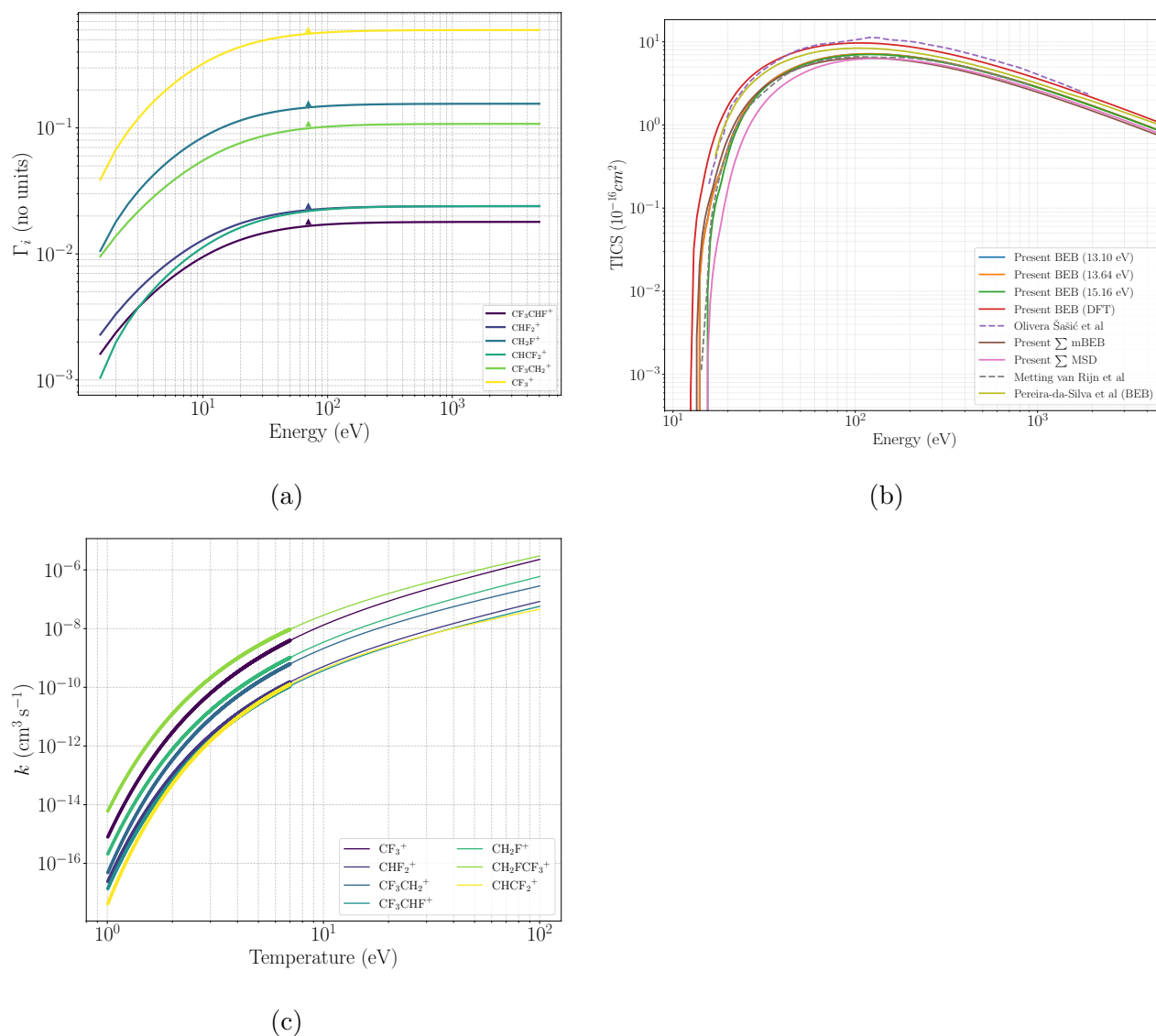


Figure 6: a) Branching ratios of 1,1,1,2-Tetrafluoroethane CH_2FCF_3 : The solid lines represent the branching ratios calculated for the MSD method, whereas the solid triangles denote the branching ratios calculated from the EIMS. b) TICS of 1,1,1,2-Tetrafluoroethane: The solid blue lines represent the TICS where the HOMO energy is 13.64 eV, the solid orange lines denote the TICS where the HOMO energy is set to 15.16 eV, the solid green line shows the TICS calculated using the DFT parameters, The solid red line indicates the sum of all PICS from the mBEB method, the solid purple line represents the sum of all PICS calculated from the MSD method. The dashed brown line represents the TICS presented by Marnik Metting van Rijn et al [10], and the solid pink line represents the TICS calculated by Pereira-da-Silva et al [25]. c) 1,1,1,2-tetrafluoroethane rate coefficients for ionization and dissociation processes, here the bold lines are the rates calculated using the MVD and the thin solid lines are the extrapolated values calculated using the Arrhenius function from 1 eV to 100 eV.

would also help us determine characteristics of the smaller fragments (< 20 amu) including the C_2^+ , C^+ and H_2^+ and the larger fragments such as the CF_x^+ ($x = 2, 3$). In Figure 8a, we have shown the branching ratios as a function of incident energy (E), the solid lines represent the continuous branching ratios used in the MSD method and the upright triangles are the BRs from the EIMS data, measured at a particular incident energy of 70 eV. In Figure 8b, and Figure 8c we have shown the TICS calculated using orbital parameters calculated using the \mathcal{HF} and the DFT level of theory. As our binding energy calculations using the \mathcal{HF} method did not yield an ionization energy§ closer to the experimental value or the value reported in the literature, we replaced our HOMO energy (15.39 eV) to 13.3 eV, which was reported in the NIST web book. The DFT calculation yielded a HOMO energy value of 12.58 eV which is closer to the value in the NIST Web book. This difference in the HOMO energy affects the magnitude and the starting point (ionization threshold) of the TICS profiles, which can be seen in Figure 8b. A similar trend can be noticed in the TICS calculated from the sum of PICS obtained from the mBEB and MSD methods, since for a few cations, their appearance energies are lesser than the ionization energies. In Figure 8c, we have shown the rates calculated using Maxwell’s electron velocity distribution (MVD) function from 1 eV till 7 eV and fitted using the Arrhenius function from 1 eV till 100 eV, the fitting constants such as A, n and E_{act} have been presented in Table 5.

§ According to Koopman’s theorem $IE = -HOMO$

4.4. 1,1,1-Trifluoropropane & 3,3,3-Trifluoropropene

1,1,1-Trifluoropropane molecule’s mass spectrum and AEs were also obtained from the work of Steele and Stone [24]. There are no previous reports on ionization potential along with ionization cross sections studies on the molecule in the literature to the best of our knowledge. From Table 1, it can be seen that our HOMO energy calculated using \mathcal{HF} method is 11.42 eV and that calculated using DFT method is 10.69 eV. The calculated BRs, PICS, and fitting parameters are shown in Table 6. In Figure 9, we have shown the PICS for the cations detected in the mass spectrum. The $C_2H_5^+$ had the most intense peak having an AE of 12.82 eV. The BRs have also been shown on Figure 10a. The TICS calculated using the parameters obtained from the \mathcal{HF} and the DFT method have been plotted in Figure 10b, and the Figure 10c, the fitting parameters have been shown in Table 6.

Similarly, 3,3,3-Trifluoropropene was also studied by Stone and Steele, and mass spectrum and AEs were provided [24]. The reported IE is 11.24 ± 0.04 eV. Our calculated HOMO values by the DFT and \mathcal{HF} methods are 12.16 eV and 14.22 eV. The Figure 11, contains the PICS calculated for all the cationic fragments presented in Table 7. Here the $C_2H_3^+$ is the most abundant fragment having an AE of 14.20 eV. The parent fragment $C_2H_3CF_3^+$ was also detected in the mass spectrum having an RI $> 60\%$. The BR has been shown in Figure 12a, where the solid lines represent the continuous BRs and the upright triangle represents the experimental BR at 70 eV. The TICS calculated using the parameters from the various methods have been shown in the Figure 12b, the HOMO energy obtained from the \mathcal{HF} method is quite

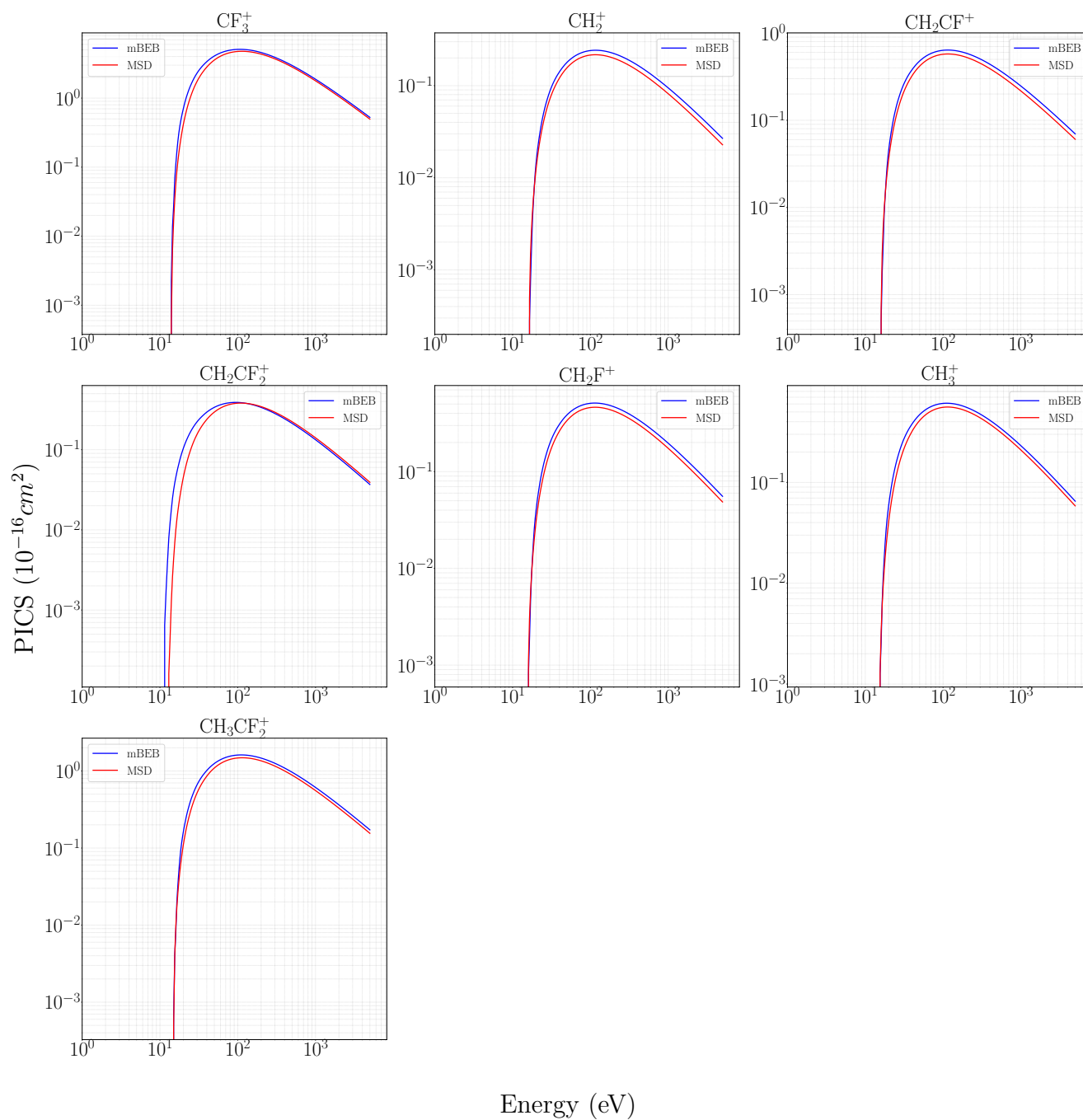


Figure 7: PICS of 1,1,1-Trifluoroethane: the cations detected in the EIMS, the blue solid line represents the calculated cross sections using the mBEB model, and the solid red line represents the calculated cross sections using the MSD method.

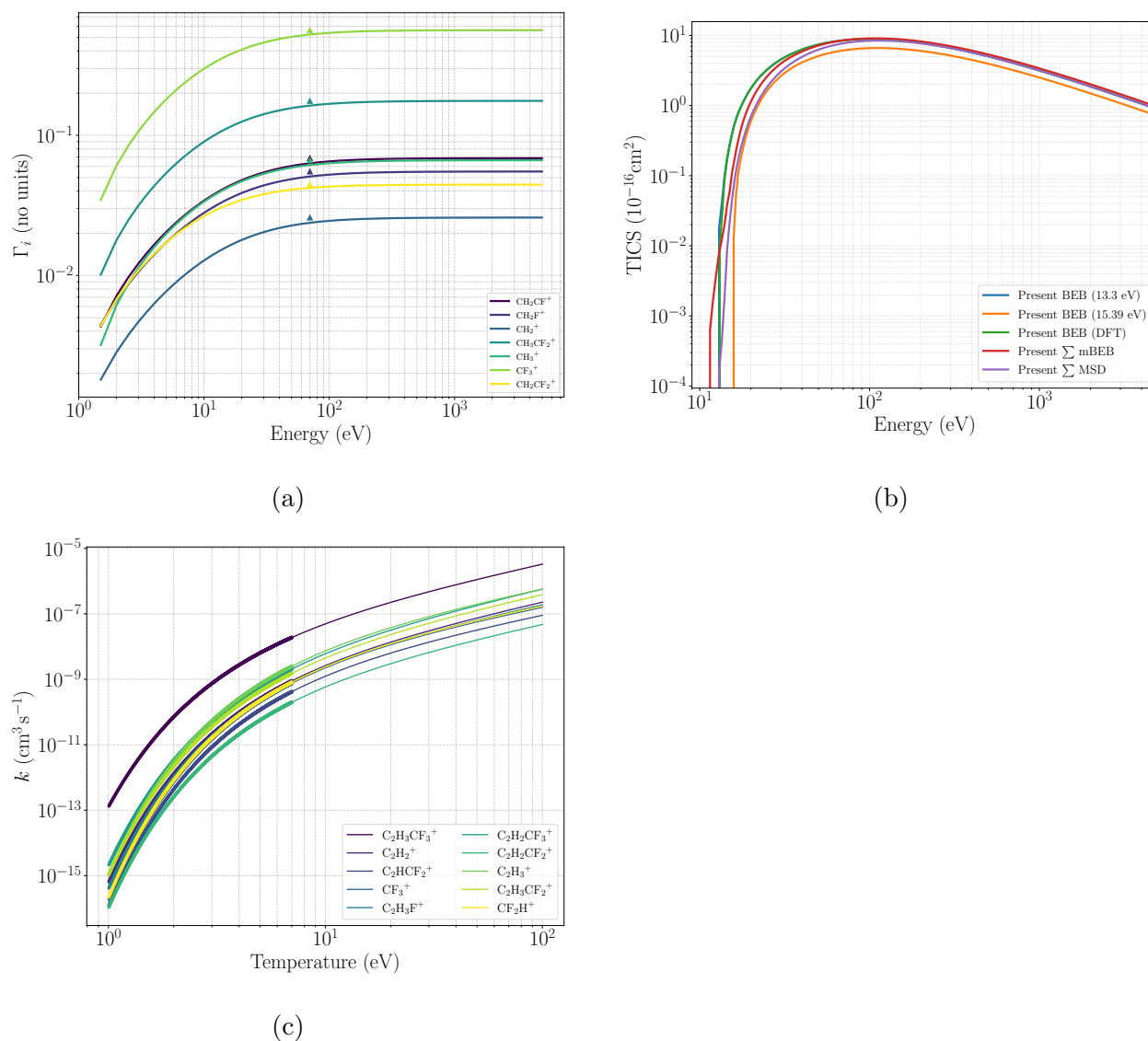


Figure 8: a) Branching ratios of 1,1,1-Trifluoroethane (CH_3CF_3): The solid lines represent the branching ratios calculated for the MSD method, whereas the solid triangles denote the branching ratios calculated from the EIMS. b) Comparison of TICS of 1,1,1-Trifluoroethane calculated using different methods, the solid blue line represents our calculated BEB TICS where the experimental first ionization energy was used, the solid orange line shows the present BEB TICS calculated using HOMO energy obtained by HF approximation, the green line represents the TICS calculated using the DFT parameters, the red line represents the sum of mBEB PICS, the purple line represents the sum of PICS calculated using the MSD method. c) 1,1,1-Trifluoroethane rate coefficients for ionization and dissociation processes, here the bold lines are the rates calculated using the MVD, and the thin solid lines are the extrapolated values calculated using the Arrhenius function from 1 eV to 100 eV.

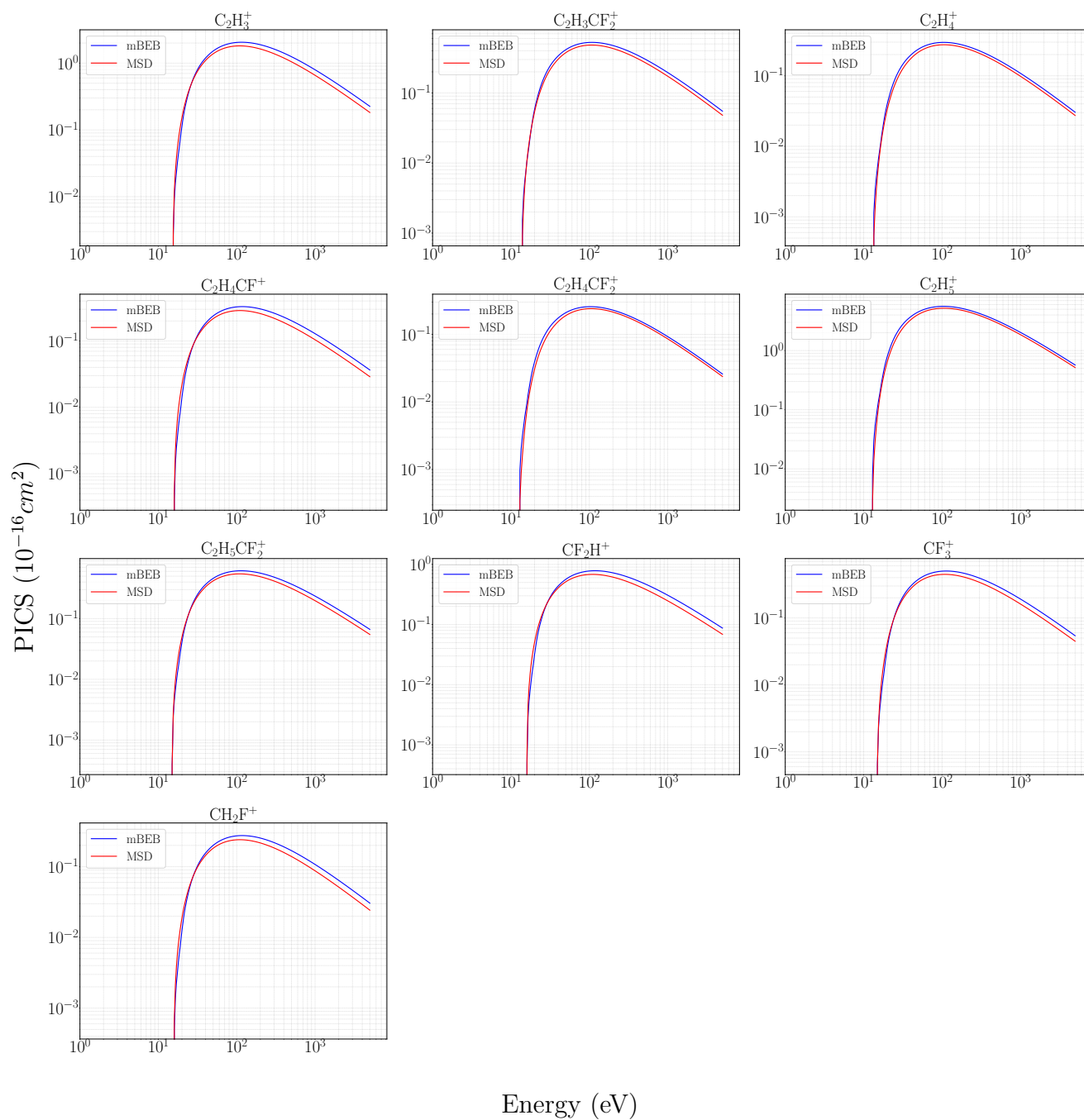
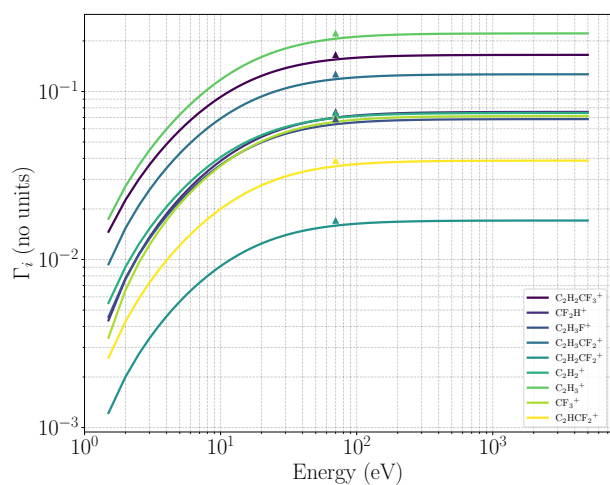
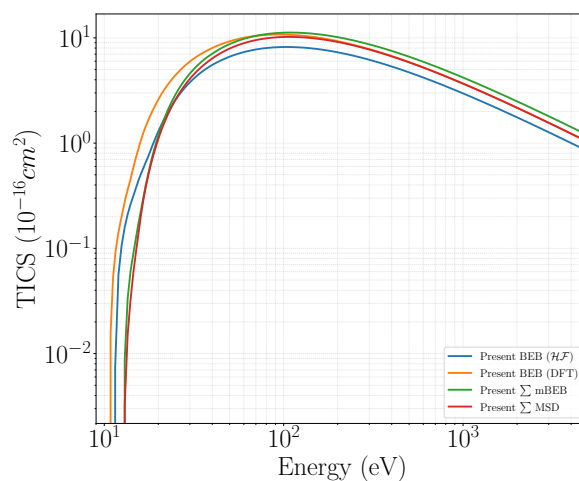


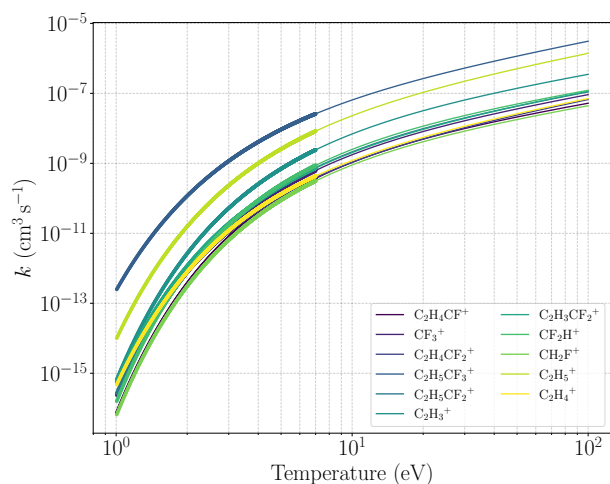
Figure 9: PICS of 1,1,1-Trifluoropropane: cations detected in the EIMS, the blue solid line represents the calculated cross sections using the mBEB model, and the solid red line represents the calculated cross sections using the MSD method.



(a)



(b)



(c)

Figure 10: a) Branching ratios of 1,1,1-Trifluoropropane ($C_2H_5CF_3$): The solid lines represent the branching ratios calculated for the MSD method, whereas the solid triangles denote the branching ratios calculated from the EIMS. b) 1,1,1-Trifluoropropane: TICS calculated using different methods, the solid blue line represents our calculated BEB TICS calculated using HOMO energy obtained by HF approximation, and the solid orange line shows the present BEB TICS calculated using orbital energies obtained by DFT method, the solid green line represents the sum of all PICS calculated from the mBEB method, the solid red line represents the PICS calculated using the MSD method. c) 1,1,1-Trifluoropropane rate coefficients for ionization and dissociation processes, here the bold lines are the rates calculated using the MVD, and the thin solid lines are the extrapolated values calculated using the Arrhenius function from 1 eV to 100 eV.

Table 5: The Appearance Energy (AE), Branching ratios (BR), cross section's maximum value (σ), the values of pre-exponent (A), scaling term (n) and the activation energy (E_{act}) of 1,1,1 Trifluoroethane (CH_3CF_3)

m/z	Cation	AE (eV)	BR	σ (10^{-16}cm^2)	A($10^{-10}\text{cm}^3\text{s}^{-1}$ eV $^{-n}$)	n	E_{act} (eV)
69	CF_3	13.9 ± 0.03	0.56 306	3.6606	18.34	1.4678	14.7157
65	CH_3CF_2	14.9 ± 0.2	0.17 623	1.1407	6.806	1.3972	15.3955
64	CH_2CF_2	11.2 ± 0.1	0.04 448	0.2924	1.330	1.513	13.7573
45	CH_2CF	15.8 ± 0.2	0.06 869	0.4428	3.060	1.3399	16.0405
33	CH_2F	15.6 ± 0.2	0.05 518	0.3560	2.391	1.3508	15.8997
15	CH_3	15.0 ± 0.1	0.06 644	0.4298	2.628	1.3875	15.4783
14	CH_2	16.2 ± 0.3	0.02 590	0.1666	1.233	1.3138	16.3484
84	CH_3CF_3	13.3 ± 0.1	–	6.7843	52.16	1.3415	13.3577

Table 6: The Appearance Energy (AE), Branching ratios (BR), cross section's maximum value (σ), the values of pre-exponent (A), scaling term (n) and the activation energy (E_{act}) of 1,1,1 Trifluoropropane ($\text{C}_2\text{H}_5\text{CF}_3$)

m/z	Cation	AE (eV)	BR	σ (10^{-16}cm^2)	A($10^{-10}\text{cm}^3\text{s}^{-1}$ eV $^{-n}$)	n	E_{act} (eV)
79	$\text{C}_2\text{H}_5\text{CF}_2$	14.9 ± 0.2	0.05 369	0.4180	6.952	1.1321	14.8573
78	$\text{C}_2\text{H}_4\text{CF}_2$	12.53 ± 0.04	0.02 330	0.1834	2.007	1.2886	12.8908
77	$\text{C}_2\text{H}_3\text{CF}_2$	13.6 ± 0.1	0.04 711	0.3690	4.892	1.2154	13.7399
69	CF_3	14.8 ± 0.1	0.04 407	0.3432	5.582	1.1404	14.7586
59	$\text{C}_2\text{H}_4\text{CF}$	15.8 ± 0.1	0.02 836	0.2199	4.249	1.0788	15.6748
51	CF_2H	15.9 ± 0.1	0.06 737	0.5220	10.32	1.0705	15.7796
33	CH_2F	15.7 ± 0.3	0.02 380	0.1846	3.511	1.0844	15.5825
29	C_2H_5	12.82 ± 0.02	0.50 658	3.9826	45.60	1.2712	13.1025
28	C_2H_4	13.0 ± 0.2	0.02 684	0.2109	2.528	1.2534	13.267
27	C_2H_3	15.3 ± 0.1	0.17 882	1.3895	24.64	1.1093	15.2106
98	$\text{C}_2\text{H}_5\text{CF}_3$	11.42	–	8.1920	103.3	1.2614	10.6984

high compared to the experimental values hence there is a shift near the threshold of the cross sections, whereas when we replace the HOMO energy value with parameters obtained by DFT method, the cross section profile begins at a lower threshold value and a higher magnitude when compared with the TICS calculated using the \mathcal{HF} method. The TICS

obtained by summing all the PICS of the cations from the MSD and the mBEB methods are in good agreement with the BEB TICS calculated using the \mathcal{HF} approximation for orbital parameters. The rate coefficients for the PICS and TICS are shown in Figure 12c, the rates were calculated using the MVD from 1 eV till 7 eV and fitted using the Arrhenius

function from 1 eV till 100 eV.

5. Conclusion

The electron impact PICS have been successfully calculated for the cations of several molecules are reported in the article. The PICS was computed using the mBEB and the MSD models. These models require the TICS, which is calculated using the BEB model. All the molecules that are studied in this article were optimised using the DFT functional (ω B97XD) and the aug-cc-PVTZ basis set. The orbital binding and kinetic energies were calculated using the \mathcal{HF} and DFT approximations using the same aug-cc-PVTZ basis set. Since the HOMO energies of all the molecular targets were high, we replaced them with the experimental IPs which are compared in Table 1 with our HOMO energy. The computed cross sections have been used to calculate the thermal rate constants for the ionization and dissociative ionization processes. Our results for molecules like trifluoromethane and 1,1,1,2-tetrafluoroethane showed good agreement with the literature data and are quite well studied. As seen in Figure 4b, our TICS compares very well with the experimental data of Torres et al [34], Kawaguchi et [37], the recommended cross sections of Christophorou et al [36], and the theoretical calculation of Kim et al [34]. However, the molecules such as 1,1,1-Trifluoroethane, 1,1,1-Trifluoropropane and 3,3,3-Trifluoropropene do not have any ionization studies in the literature and hence this study provides a comprehensive data for these targets for the first time. Also we have found that the agreement between the activation energy and appearance energy is linear as can be observed from tables 2 to 7. However, no direct functional dependence or correlation is available. Our opinion is that revisit-

ing these molecules with the current apparatus will provide a more comprehensive investigation of these targets. Finally, a comparison of all the TICS and their total ionization rate constants have been shown in Figure 13 where normally with the size of the target the TICS increases.

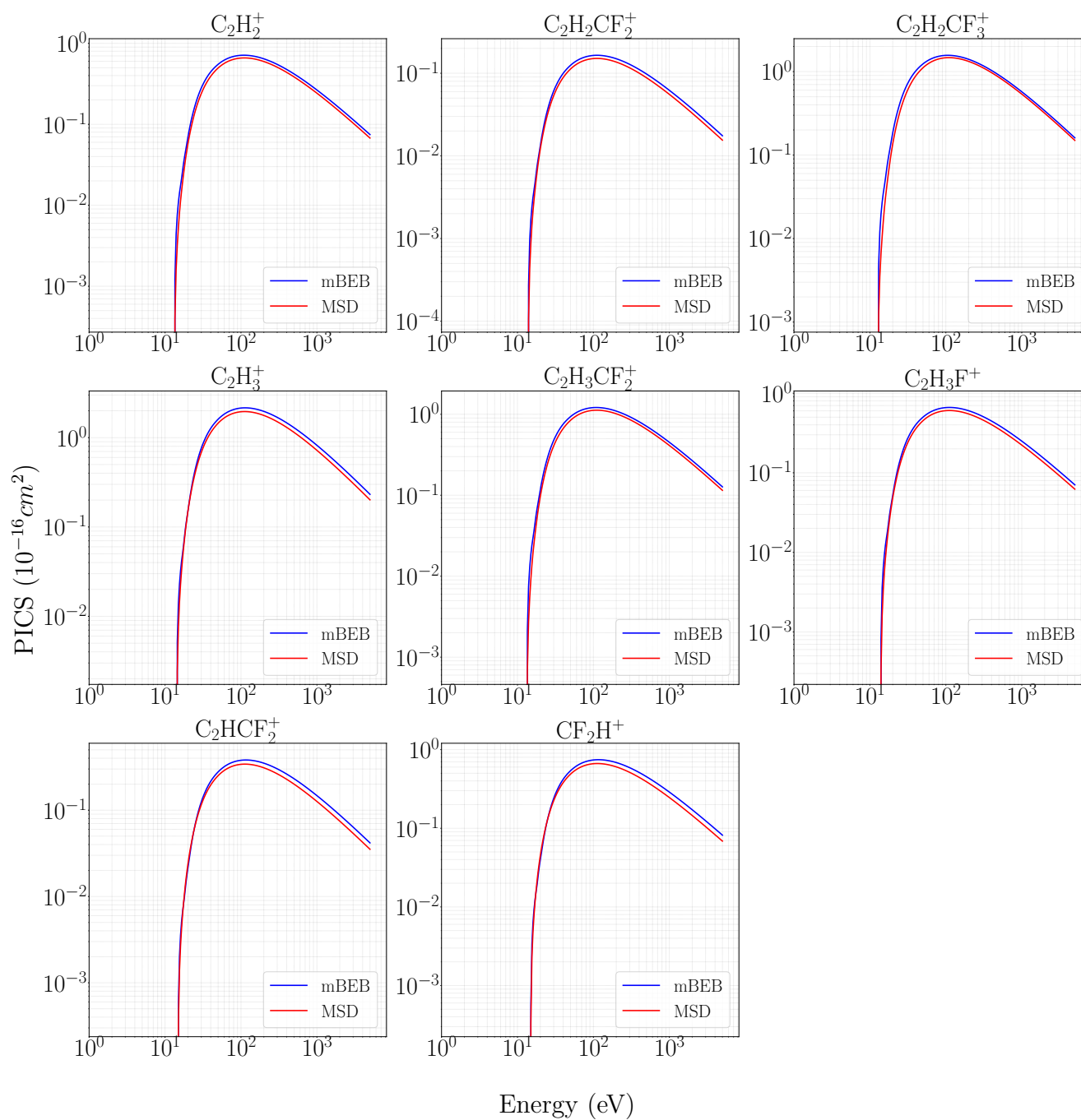


Figure 11: PICS of 3,3,3-Trifluoropropene: cations detected in the EIMS, the blue solid line represents the calculated cross sections using the mBEB model, and the solid red line represents the calculated cross sections using the MSD method.

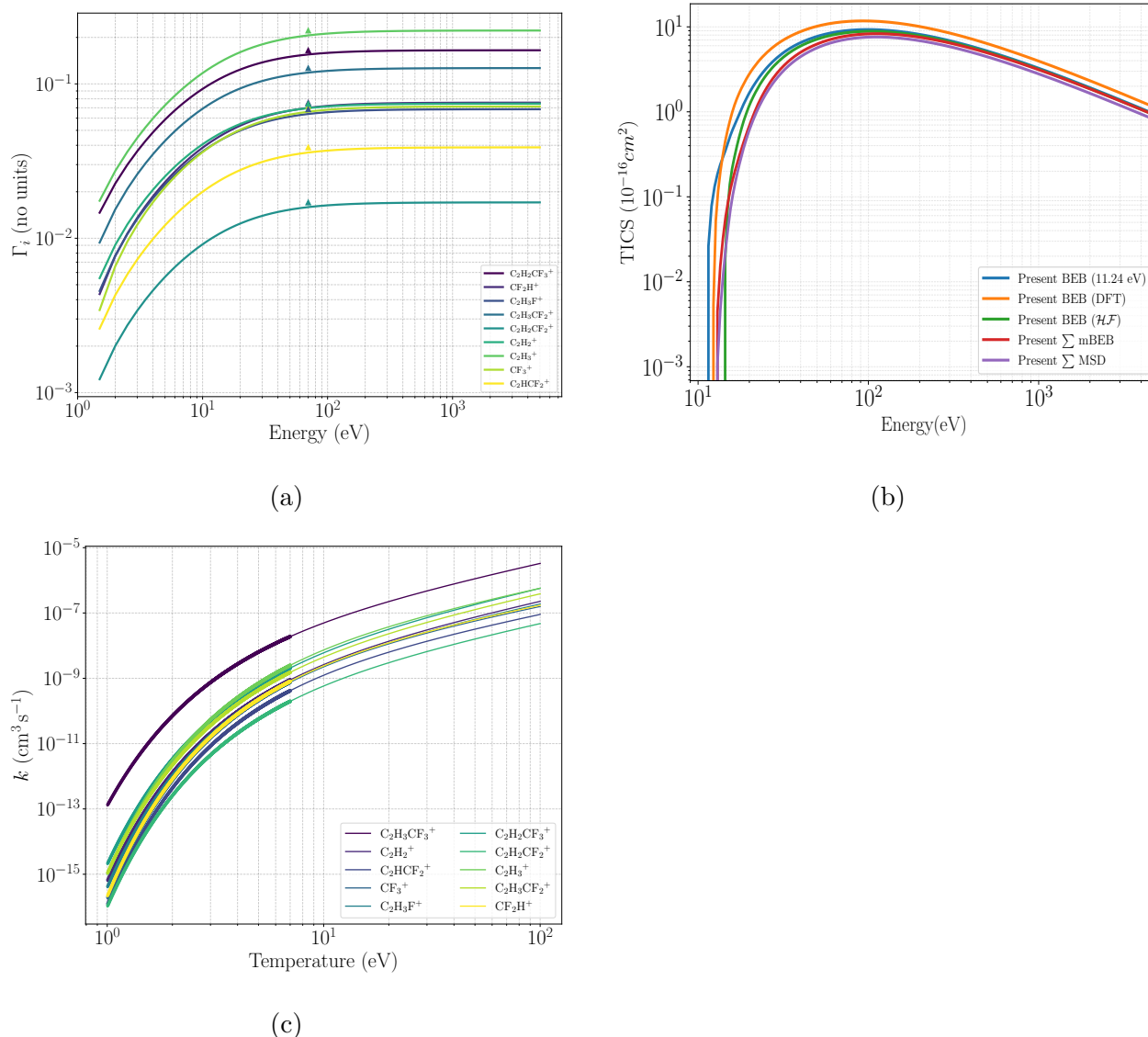
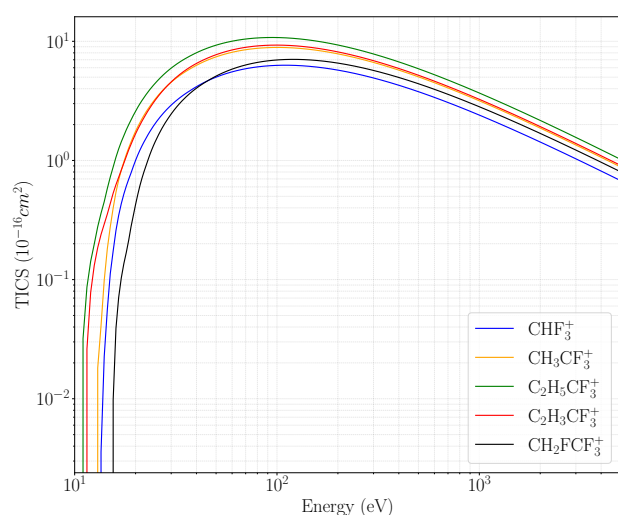


Figure 12: a) Branching ratios of 3,3,3-Trifluoropropene $C_3H_3CF_3$: The solid lines represent the branching ratios calculated for the MSD method, whereas the solid triangles denote the branching ratios calculated from the EIMS. b) 3,3,3-Trifluoropropene: TICS calculated using different methods, the solid blue line represents our calculated BEB TICS where the experimental first ionization energy was used, and the solid orange line shows the present BEB TICS calculated using values obtained from the DFT method, the solid green line shows the present BEB TICS calculated using HOMO energy obtained by HF approximation, the red lines represents the sum of PICS calculated from the mBEB method, and the purple lines show the sum of PICS calculated from the MSD method. c) 3,3,3-Trifluoropropene rate coefficients for ionization and dissociation processes, here the bold lines are the rates calculated using the MVD, and the thin solid lines are the extrapolated values calculated using the Arrhenius function from 1 eV to 100 eV.

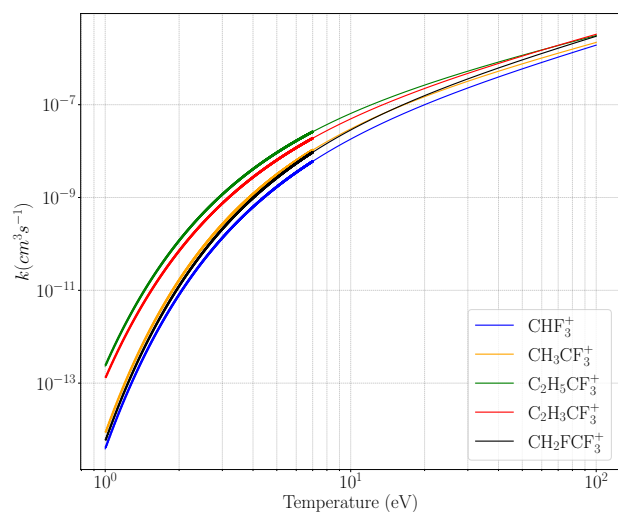
Table 7: The Appearance Energy (AE), Branching ratios (BR), cross section's maximum value (σ), the values of pre-exponent (A), scaling term (n) and the activation energy (E_{act}) of 3,3,3 Trifluoropropane ($C_2H_3CF_3$)

m/z	Cation	AE (eV)	BR	σ ($10^{-16}cm^2$)	A($10^{-10}cm^3s^{-1} eV^{-n}$)	n	E_{act} (eV)
95	$C_2H_2CF_3$	12.69 ± 0.05	0.16	515	1.4696	7.322	1.4747 12.8115
77	$C_2H_3CF_2$	13.3 ± 0.15	0.12	657	1.1230	6.487	1.4163 13.3467
76	$C_2H_2CF_2$	13.8 ± 0.1	0.01	706	0.1510	98.24	1.3716 13.7944
75	C_2HCF_2	14.8 ± 0.2	0.03	879	0.3416	2.785	1.2877 14.7085
69	CF_3	15.0 ± 0.2	0.07	138	0.6279	5.444	1.2644 14.9268
51	CF_2H	14.9 ± 0.1	0.07	559	0.6653	5.573	1.2774 14.8112
46	C_2H_3F	13.85 ± 0.02	0.06	849	0.6061	3.994	1.3666 13.8423
27	C_2H_3	14.20 ± 0.05	0.22	168	1.9580	13.97	1.337 14.1573
26	C_2H_2	13.3 ± 0.15	0.07	448	0.6608	3.818	1.4163 13.3467
96	$C_2H_3CF_3$	11.24 ± 0.04	–	9.2915		56.96	1.4043 10.7188

- [1] LL Alves, A Bogaerts, V Guerra, and MM Turner. Foundations of modelling of nonequilibrium low-temperature plasmas. *Plasma Sources Science and Technology*, 27(2):023002, 2018.
- [2] Jane L Fox. Aeronomy. In *Springer handbook of atomic, molecular, and optical physics*, pages 1299–1336. Springer, 1996.
- [3] Leon Sanche. Low energy electron-driven damage in biomolecules. *The European Physical Journal D-Atomic, Molecular, Optical and Plasma Physics*, 35:367–390, 2005.
- [4] Sara A Zein, Marie-Claude Bordage, Ziad Francis, Giovanni Macetti, Alessandro Genoni, Claude Dal Cappello, Wook-Geun Shin, and Sebastien Incerti. Electron transport in dna bases: An extension of the geant4-dna monte carlo toolkit. *Nuclear Instruments and Methods in Physics Research Section B: Beam Interactions with Materials and Atoms*, 488:70–82, 2021.
- [5] G. Saviano, M. Ferrini, L. Benussi, S. Bianco, D. Piccolo, S. Colafranceschi, J. KjØlbro, A. Sharma, D. Yang, G. Chen, Y. Ban, Q. Li, S. Grassini, and M. Parvis. Properties of potential eco-friendly gas replacements for particle detectors in high-energy physics. *Journal of Instrumentation*, 13(03):P03012, mar 2018.
- [6] JM John, G Majumder, and S Pethuraj. Simulation of rpc responses in mini-iron calorimeter for cosmic ray muon studies. *Journal of Instrumentation*, 18(11):P11023, 2023.
- [7] Bashar Al Atoum, Steve F Biagi, Diego González-Díaz, Ben JP Jones, and Austin D McDonald. Electron transport in gaseous detectors with a python-based monte carlo simulation code. *Computer Physics Communications*, 254:107357, 2020.
- [8] SF Biagi. Monte carlo simulation of electron drift and diffusion in counting gases under the influence of electric and magnetic fields. *Nuclear Instruments and Methods in Physics Research Section A: Accelerators, Spectrometers, Detectors and Associated Equipment*, 421(1-2):234–240, 1999.
- [9] Ryan Park, Brett Scheiner, and Mark Christian Zammit. Thunderboltz: An open-source direct simulation monte carlo boltzmann solver for plasma transport, chemical kinetics, and 0d modeling. *Plasma Sources Science and Technology*, 2024.
- [10] Marnik Metting van Rijn, Stephen F Biagi, and Christian Franck. Electron scattering cross sections of 1, 1, 1, 2-tetrafluoroethane (r134a). *Journal of Physics D: Applied Physics*, 57(35):355202, 2024.
- [11] GJM Hagelaar. Brief documentation of bolsig+ version 03/2016. *Laboratoire Plasma et Conversion d’Energie (LAPLACE), Universit Paul Sabatier*, 118, 2016.
- [12] Dhanoj Gupta, Heechol Choi, Mi-Young Song, Grzegorz P Karwasz, and Jung-Sik Yoon.



(a)



(b)

Figure 13: The total electron impact ionization cross sections and the ionization rate constants of all the molecules discussed in the manuscript.

Electron impact ionization cross section studies of C_2F_x ($x = 1-6$) and C_3F_x ($x = 1-8$) fluorocarbon species. *The European Physical Journal D*, 71:1–10, 2017.

- [13] Suriyaprasanth Shanmugasundaram, Rounak Agrawal, and Dhanoj Gupta. Electron impact partial ionization cross sections: R-carvone, 2-butanol, imidazole, and 2-nitroimidazole. *The Journal of Chemical Physics*, 160(9), 2024.

- [14] Yong-Ki Kim and M Eugene Rudd. Binary-encounter-dipole model for electron-impact ionization. *Physical Review A*, 50(5):3954, 1994.
- [15] RCSB PDB: Chemical Sketch Tool – rcsb.org. <https://www.rcsb.org/chemical-sketch>. [Accessed 20-07-2024].
- [16] Jeroen Koopman and Stefan Grimme. From qceims to qcxms: A tool to routinely calculate cid mass spectra using molecular dynamics. *Journal of the American Society for Mass Spectrometry*, 32(7):1735–1751, 2021.
- [17] Stefan E Huber, Andreas Mauracher, Daniel Süß, Ivan Sukuba, Jan Urban, Dmitry Borodin, and Michael Probst. Total and partial electron impact ionization cross sections of fusion-relevant diatomic molecules. *The Journal of Chemical Physics*, 150(2), 2019.
- [18] RK Janev and D Reiter. Collision processes of C_2 , C_3 and C_2H hydrocarbons with electrons and protons. *Physics of Plasmas*, 11(2):780–829, 2004.
- [19] Vincent Graves, Bridgette Cooper, and Jonathan Tennyson. Calculated electron impact ionisation fragmentation patterns. *Journal of Physics B: Atomic, Molecular and Optical Physics*, 54(23):235203, 2022.
- [20] Sharon G. Lias. Ionization energy evaluation. *NIST Chemistry WebBook, NIST Standard Reference Database Number 69*. (Retrieved July 16, 2024).
- [21] W.R. Harshbarger, M.B. Robin, and E.N. Lassettre. The electron impact spectra of the fluoromethanes. *Journal of Electron Spectroscopy and Related Phenomena*, 1:319, 1973.
- [22] Peter J Linstrom and William G Mallard. The nist chemistry webbook: A chemical data resource on the internet. *Journal of Chemical & Engineering Data*, 46(5):1059–1063, 2001.
- [23] JM Simmie and E Tschuikow-Roux. Mass spectrum, appearance potentials and bond dissociation energies of 1, 1, 1-trifluoroethane. *International Journal of Mass Spectrometry and Ion Physics*, 7(1):41–45, 1971.
- [24] WC Steele and FCA Stone. An electron impact study of 1, 1, 1-trifluoroethane, 1, 1, 1-trifluoropropane and 3, 3, 3-trifluoropropene. *Journal of the American Chemical Society*, 84(18):3450–3454, 1962.
- [25] João Pereira-da Silva, Rodrigo Rodrigues, Joao

- Ramos, Carlos Brígido, Alexandru Botnari, Miguel Silvestre, João Ameixa, Mónica Mendes, Fábio Zappa, Stephen J Mullock, et al. Electron driven reactions in tetrafluoroethane: Positive and negative ion formation. *Journal of the American Society for Mass Spectrometry*, 32(6):1459–1468, 2021.
- [26] Weidong Zhou, DP Seccombe, and RP Tuckett. Fragmentation of valence electronic states of $\text{cf}^+ 3\text{-ch}^+ 2\text{f}^+$ and $\text{chf}^+ 2\text{-chf}^+ 2^+$ in the range 12–25 eV. *Physical Chemistry Chemical Physics*, 4(19):4623–4633, 2002.
- [27] Masashi Goto, Keiji Nakamura, Hirotaka Toyoda, Hirotaka Toyoda, and Hideo Sugai. Cross section measurements for electron-impact dissociation of chf_3 into neutral and ionic radicals. *Japanese journal of applied physics*, 33(6R):3602, 1994.
- [28] Don L Hobrock and Robert W Kiser. Electron impact studies of some trihalomethanes: Trichloromethane, dichlorofluoromethane, chlorodifluoromethane, and trifluoromethane. *The Journal of Physical Chemistry*, 68(3):575–579, 1964.
- [29] H Sugai, H Toyoda, T Nakano, and M Goto. Absolute cross sections for the electron-impact dissociation of cf_4 and chf_3 into the cf_x ($x=1-3$) neutral radicals. *Contributions to Plasma Physics*, 35(4-5):415–420, 1995.
- [30] Charles Q Jiao, Rajesh Nagpal, and Peter D Haaland. Ion chemistry in trifluoromethane, chf_3 . *Chemical physics letters*, 269(1-2):117–121, 1997.
- [31] Ione Iga, Ivana P Sanches, Santosh Kumar Srivastava, and Michael Mangan. Electron impact ionization of chf_3 . *International Journal of Mass Spectrometry*, 208(1-3):159–167, 2001.
- [32] Inmaculada Torres, Roberto Martínez, and Fernando Castaño. Electron-impact dissociative ionization of fluoromethanes chf_3 and cf_4 . *Journal of Physics B: Atomic, Molecular and Optical Physics*, 35(11):2423, 2002.
- [33] U Onthong, H Deutsch, K Becker, S Matt, M Probst, and TD Märk. Calculated absolute electron impact ionization cross-section for the molecules cf_3x ($x= \text{h, br, i}$). *International Journal of Mass Spectrometry*, 214(1):53–56, 2002.
- [34] I Torres, R Martinez, MN Sánchez Rayo, and F Castaño. Evaluation of the computational methods for electron-impact total ionization cross sections: Fluoromethanes as benchmarks. *The Journal of chemical physics*, 115(9):4041–4050, 2001.
- [35] BL Peko, RL Champion, MVVS Rao, and James K Olthoff. Measured cross sections and ion energies for a chf_3 discharge. *Journal of applied physics*, 92(3):1657–1662, 2002.
- [36] Loucas G Christophorou and James K Olthoff. Electron interactions with chf_3 , cf_3i , and $\text{c-cf}_4\text{f}_8$. In *Fundamental Electron Interactions with Plasma Processing Gases*. 2004.
- [37] Satoru Kawaguchi, Kohki Satoh, and Hidenori Itoh. Electron collision cross sections of chf_3 and electron transport in chf_3 and chf_3 -ar mixtures. *Japanese Journal of Applied Physics*, 54(1S):01AC01, 2014.
- [38] W Lowell Morgan, Carl Winstead, and Vincent McKoy. Electron cross section set for chf_3 . *Journal of Applied Physics*, 90(4):2009–2016, 2001.
- [39] Scipy curve fit.
- [40] Deepak Bose, MVVS Rao, TR Govindan, and M Meyyappan. Uncertainty and sensitivity analysis of gas-phase chemistry in a chf_3 plasma. *Plasma sources science and technology*, 12(2):225, 2003.
- [41] Vítor SA Bonfim, Cauê P Souza, Daniel AB de Oliveira, Leonardo Baptista, Antônio CF Santos, and Felipe Fantuzzi. Deciphering the irradiation induced fragmentation-rearrangement mechanisms in valence ionized $\text{cf}_3\text{ch}_2\text{f}$. *The Journal of chemical physics*, 160(12), 2024.
- [42] Toshio Hayashi, Kenji Ishikawa, Makoto Sekine, and Masaru Hori. Dissociative properties of 1, 1, 1, 2-tetrafluoroethane obtained by computational chemistry. *Japanese Journal of Applied Physics*, 57(6S2):06JC02, 2018.